© 1994, CIVIL-COMP Ltd, Edinburgh, Scotland
M. Papadrakakis and B.H.V. Topping (Editors),
Advances in Computational Mechanics, 253-261

IMPLEMENTATION AND PERFORMANCE OF ARNOLDI AND LANCZOS EIGENSOLVERS IN GALERKIN-FINITE ELEMENT COMPUTATIONS

D. Papadopoulos* , C. Siettos* , A.G. Boudouvis* and A.T. Chronopoulos✻
*** Department of Chemical Engineering, National Technical University of Athens, Athens, Greece**
✻Department of Computer Science, University of Minnesota, Minneapolis, United States of America

Abstract

The methods of Arnoldi and Lanczos are implemented for solving large and sparse eigenvalue problems. Such problems arise in the computation of stability of solutions of parameter-dependent, nonlinear partial differential equations discretized by the Galerkin/finite element method. Results are presented for the stability of equilibrium solutions of axisymmetric ferromagnetic liquid interfaces in external magnetic field of varying strength.

1 Introduction

Many important scientific and engineering problems require the computation of a small number of eigenvalues and their corresponding eigenvectors of large and sparse matrices such as those arising in the discretization of nonlinear, time dependent partial differential equations by Galerkin's method of weighted residuals and finite element basis functions. The wanted eigenvalues are in most cases in the extreme part of the matrix eigenspectrum, i.e. those with the algebraically largest and smallest real parts. These eigenvalues determine the stability of solutions, that is the outcome of the competition between a base state -- an equilibrium state in this work -- of a system and ever-present disturbances of infinitesimal (practically small) amplitude.

The equations are discretized by nicely suited finite element basis functions and Galerkin's method of weighted residuals, which reduces the original partial differential equation system to a large system of ordinary differential equations $\underline{R}(\underline{y}, \dot{\underline{y}}\ ; p) = \underline{0}$, where $\underline{R}$ is the set of residuals, $\underline{y}$ is the set of values of the unknowns at the nodes of the discretization (nodal values) and $\dot{\underline{y}}$ their time derivatives, and p is a relevant parameter (or a set of them). Equilibrium solutions $\underline{y}_0$ satisfy the nonlinear system $\underline{R}(\underline{y}_0, \underline{0}; p) = \underline{0}$, which is solved by Newton iteration with parameter continuation.

Stability is governed by the system linearized for small disturbances $\delta\underline{y}$ from $\underline{y}_0$, the time dependence of which can be taken as exponential. Thus $\delta\dot{\underline{y}} = \lambda\delta\underline{y}$ and stability is governed by a linearized eigenproblem ([1])

$$\delta\underline{R} = \underline{R}_{\underline{y}}\delta\underline{y} + \underline{R}_{\dot{\underline{y}}}\lambda\delta\underline{y} = \underline{0}, \quad \text{i.e.} \quad \underline{\underline{J}}\underline{x}_i = \lambda_i \underline{\underline{M}}\underline{x}_i \qquad (1)$$

where the eigenvectors $\underline{x}_i$ are normal mode components of $\delta\underline{y}$, $\underline{\underline{J}} \equiv \underline{R}_{\underline{y}}$ is the Jacobian matrix of the equilibrium state, $\underline{\underline{M}} \equiv -\underline{R}_{\dot{\underline{y}}}$ is the overlap or 'mass' matrix of the finite element basis functions, and the eigenvalues λ_i are the stability indicators. If any of the λ_i have positive real part, or 'growth factors', the equilibrium state is unstable to the corresponding eigenvector or mode -- and to the disturbance it carries. The eigenproblem is to be solved for the most dangerous modes, i.e. those with largest growth factors.

The generalized eigenproblem (1) is usually reduced, via appropriate matrix transformations, to the standard eigenvalue problem

$$\underline{\underline{A}}\underline{x} = \lambda\underline{x} \qquad (2)$$

which could be symmetric or nonsymmetric. Depending on the symmetry of $\underline{\underline{A}}$, different eigensolvers are used to solve (2). Arnoldi's eigensolver is appropriate for the non-symmetric case; Lanczos' for the symmetric.

It is worth mentioning that the standard eigenproblem arises directly in the computation of stability of time periodic solutions bifurcating from steady ones (Hopf bifurcation). In that case, the wanted eigenvalues are those that are about to cross the unit circle in the complex plane.

The case under study here is drawn from capillary magnetohydrostatics. The stability of equilibrium states of ferrofluid masses with free surfaces in an external magnetic field of varying strength is computed. The equilibrium equations are derived from an energy formulation (variational formulation) and the resulting Jacobian matrix is symmetric; or from a force formulation, where the equations are statements of force balances, and the resulting Jacobian matrix is nonsymmetric.

2 The case study: Magnetohydrostatic equilibria of axisymmetric ferrofluid interfaces

The situation of concern is shown in Figure 1. It is the equilibrium deformation of a laterally unbounded, axisymmetric interface between a ferromagnetic liquid, commonly known as ferrofluid, and a non-magnetic medium (e.g. air) in the presence of a magnetic field.

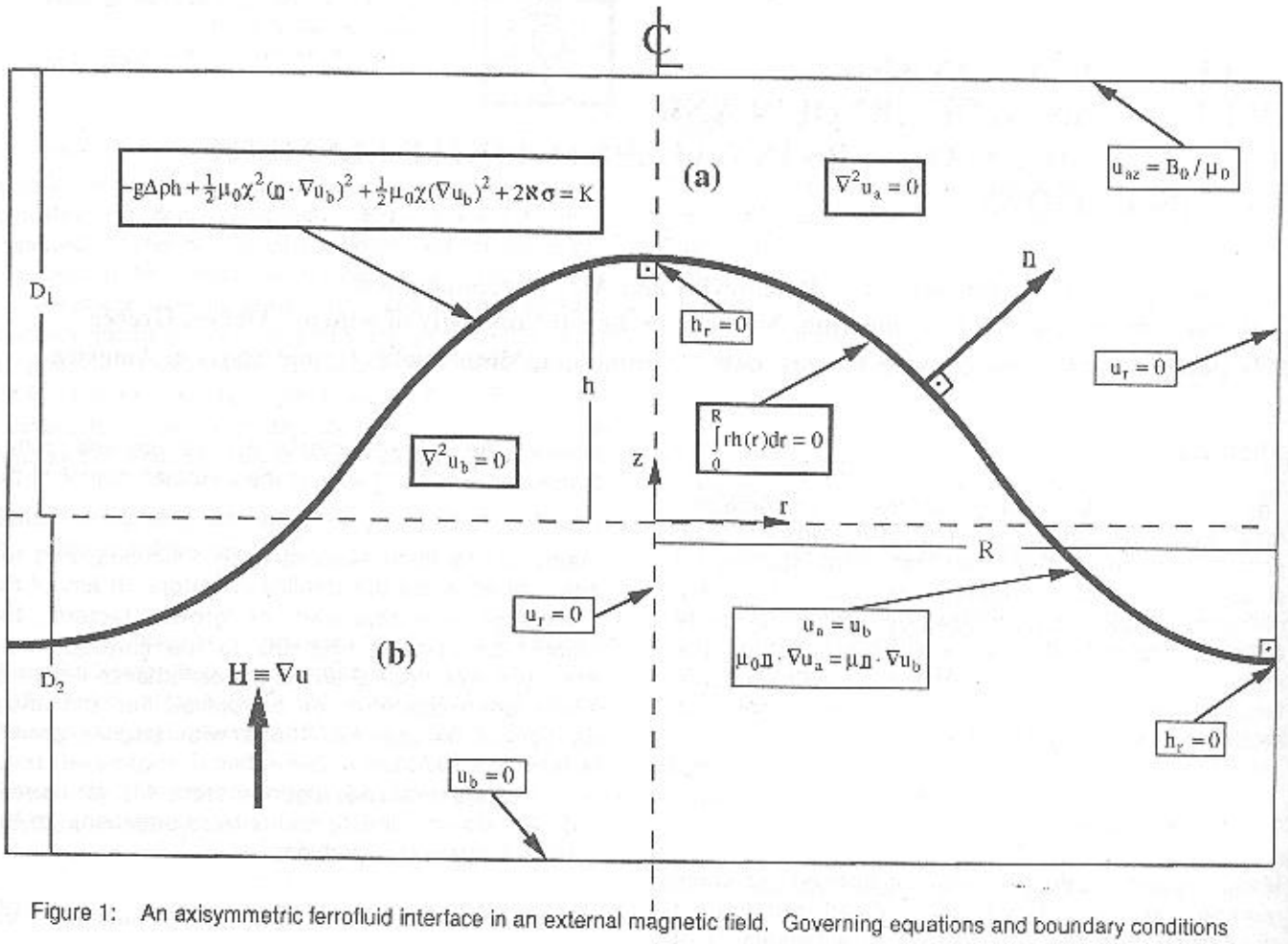

Figure 1: An axisymmetric ferrofluid interface in an external magnetic field. Governing equations and boundary conditions

In the absence of an applied field the ferrofluid interface is flat and remains flat until the strength, H_0, of an applied uniform magnetic field oriented perpendicularly to the interface reaches a critical value, $H_{0,cr}$. At $H_0 > H_{0,cr}$ the interface deforms in the direction of the field, whereas the ferrofluid underneath remains static. Distortions of the interface shape lead to deviations of the nearby magnetic field from the uniformity it displays away from the interface.

This phenomenon was first observed in confined ferrofluid interfaces by Cowley and Rosensweig [2] and it was named normal field instability. The name is suggestive of the mechanism that causes the phenomenon: the flat interface is distorted by ever-present disturbances, and flux of the applied magnetic field is concentrated at the peaks of the distorted surface; the magnetostatic forces tend to magnify any disturbance but surface tension tends to flatten the surface and eliminate the disturbance. So does gravity, when, as in the present case, the ferrofluid is below a lighter non-magnetic fluid. At the onset of the instability the destabilizing influence of magnetostatic forces exceeds the stabilizing influence provided by surface tension and gravity.

The equations governing the magnetohydrostatic equilibria of the ferrofluid interface are listed below (and displayed in Figure 1); they are derived in detail in [3] and [4].

The magnetostatic forces within the ferrofluid (phase b) are governed by Laplace's equation for the magnetostatic potential, u:

$$\nabla^2 u_b = 0 \qquad (3a)$$

The magnetostatic potential in air (phase a) also satisfies Laplace's equation:

$$\nabla^2 u_a = 0 \qquad (3b)$$

The potential u 'produces' the magnetic field, $\underline{H}$, $\underline{H} = \nabla u$. The magnetic induction, $\underline{B}$, is everywhere parallel to $\underline{H}$, $\underline{B} = \mu\underline{H}$, inside the ferrofluid, and $\underline{B} = \mu_0\underline{H}$, inside air, where μ is the magnetic permeability of the ferrofluid, taken as constant, and μ_0 is the constant in the Biot-Savart law, $\mu_0 = 4\pi \times 10^{-7}$ henry/m (SI units).

The static equilibrium shape of the interface is dictated by the requirement that magnetostatic force balances the capillary force, that is a resultant of surface tension, σ, acting in a curved interface and the hydrostatic pressure that is a resultant of gravity. Force balancing is expressed by a nonlinear partial differential equation, the magnetically augmented Young-Laplace equation of capillarity:

$$-g\Delta\rho h+\frac{1}{2}\mu_0\chi^2(\underline{n}\cdot\nabla u_b)^2+\frac{1}{2}\mu_0\chi(\nabla u_b)^2+2\aleph\sigma=K \qquad (4)$$

on z=h(r), with h(r) representing the shape of the interface; thus the gradient of the potential u_b entering Eqn. (4) is evaluated at z=h(r). g is the gravitational

acceleration, $\chi \equiv (\mu/\mu_0) - 1 > 0$ is the magnetic susceptibility of the ferrolfuid and $\Delta\rho \equiv \rho_h - \rho_a$ is the density difference between the ferrofluid and air. The unit normal $\underline{n}$ to the interface and the local mean curvature $2\aleph$ of the interface are given by

$$\underline{n} = \frac{-h_r \underline{e}_r + \underline{e}_z}{(1+h_r^2)^{1/2}} \tag{5}$$

$$2\aleph = \frac{1}{r}\frac{d}{dr}\left[\frac{rh_r}{(1+h_r^2)^{1/2}}\right] \tag{6}$$

Here the subscript r denotes differentiation in the radial direction (and the subscript z in Figure 1 differentiation in the z-direction). $\underline{e}_r$ and $\underline{e}_z$ are the unit vectors in the r- and z-direction respectively. K in Eqn. (4) is an unknown, a constant reference pressure along the interface.

The ferrofluid is incompressible and thus its volume is preserved in any interface deformation:

$$\int_0^R rh(r)dr = 0 \tag{7}$$

The undeformed (flat) ferrofluid/air interface is located at z=0; this explains why the right side of equation (7) is set to zero.

The equations are posed in a domain that is truncated both above and below the interface, i.e. $-D_2 \le z \le D_1$ (see Figure 1); D_1 and D_2 are taken large enough so that magnetic field is virtually uniform at the top and bottom boundaries of the domain. Although the ferrrofluid interface is laterally unbounded, the domain is taken to be laterally bounded. Its size in the radial direction is dictated by the wavenumber, $k_{cr} = (g\Delta\rho/\sigma)^{1/2}$, of the distorted axisymmetric interface shape at the onset of the instability ([3], [4]). The wavelength, R ($0 \le r \le R$) of the interface shape is given by $R = \lambda_1/k_{cr}$, where λ_1 is the smallest zero of the Bessel function $J_1(r)$, $\lambda_1 = 3.832$ ([4]).

The set of governing equations and boundary conditions listed above is called the *force formulation* of the magnetohydrostatic equilibria of a ferrofluid interface, because they are statements of balances of all forces that are present in the ferrofluid/air system.

An alternative formulation is the so-called energy formulation that is a statement of minimization of the total energy of the system at equilibrium. The appropriate energy functional that includes the gravitational, magnetic and interfacial energies of the system and accounts for the constraint of fixed ferrofluid volume is given by

$$\wp \equiv \tfrac{1}{2}g\Delta\rho\int_0^R h^2 r dr - \tfrac{1}{2}\mu\int_{0-D_2}^{R}\int^{h}(\nabla u_h)^2 r dr dz - \tfrac{1}{2}\mu_0\int_0^R\int_h^{D_2}(\nabla u_a)^2 r dr dz$$

$$+\sigma\int_0^R(1+h_r^2)^{1/2} r dr + K\int_0^R h r dr \tag{8}$$

and it is minimized over all admissible perturbations of h and u. The minimization of (8) over perturbations $u+\varepsilon\varphi(r,z)$ and $h+\varepsilon\xi(r)$ of u and h, respectively, is equivalent to the condition $(d\wp/d\varepsilon)|_{\varepsilon=0} = 0$. Substituting the perturbations of u and h into Eqn. (8) and requiring that the minimization condition be satisfied, we recover the governing equations and boundary conditions of the force formulation; that is, the minimizers u and h of $\wp$ are the equilibrium solutions that satisfy Eqns. (3), (4) and (7) and their boundary conditions. Therefore, force and energy formulations are equivalent.

The set of governing equations (3), (4) and (7) and their boundary conitions in the force formulation (or the equivalent energy formulation) constitute a nonlinear problem. The inherent nonlinearities arise in the Young-Laplace equation (Eqn. (4)) and they are due to the curvature term, a nonlinear function of interface location (cf. Eqn. (6)), and to the magnetic terms, which are nonlinear in the gradient of the magnetostatic potential at the interface. Furthermore the problem is a free boundary one because the interface shape is unknown a priori and must be solved for right along with the magnetostatic potential.

3 The computational problem

The problem of magnetohydrostatic equilibria of an axisymmetric ferrofluid interface so formulated as to account for the effects of gravity, surface tension and magnetic field non-uniformity, including large distortions of the interface from any simple shape, is amenable to solution only by means of modern computer-aided methods. The choice here is the combination of Galerkin's method of weigted residuals and finite element basis functions ([5]).

The domain is tessellated into quadrilateral elements between suitably placed vertical spines and transverse curves whose intersections with each spine are located at distances that are proportional to the displacement of the interface along that spine. The dependent variables u(r,z) and h(r) are then expressed in terms of finite element basis funtions that are quadratic polynomials in each spatial coordinate:

$$u(r,z) = \sum_{i=1}^{N} u_i \varphi^i(r,z) \tag{9a}$$

$$h(r) = \sum_{j=1}^{M} h_j \varphi^j(r, h(r)) \tag{9b}$$

Each basis function is unity at the i-th node created by the tessellation and zero at all other nodes. Here u_i is the value of the potential at the i-th node in the domain and h_j is the value of the interface displacement at the j-th interface node. N is the total number of nodes in the entire domain and M is the number on the interface alone.

The governing equations (3) and (4) are discretized with the Galerkin method by weighting their residuals with each basis function in turn, i.e. by multiplying each equation by each basis function separately, then substituting the unknowns from Eqns. (9), then integrating by Gauss quadrature in an isoparametric domain and setting each of the resulting equations to zero; for more details about the

implementation of the method we refer to [6] and [7], where similar situations are analyzed. Eqn. (7), being already an integral equation, is not weighted in the Galerkin sense; h is substituted from Eqn. (9b) and the integration is also done by Gauss quadrature.

The discretized problem is a set of (N+M+1) nonlinear algebraic equations in the uknowns u_i, h_j and K. In compact form it reads

$$\underline{R} \equiv [\underline{R}_p, \underline{R}_{YL}, R_{VC}] = \underline{R}(\underline{y}; p) = \underline{0} \tag{10}$$

$\underline{R}$ is the set of residuals and $\underline{R}_p, \underline{R}_{YL}, R_{vc}$ the subsets of residuals of Laplace's equation, the Young-Laplace equation and the volume constraint, respectively; $\underline{y} \equiv [\underline{u}, \underline{h}, K]$ is the set of unknowns and $\underline{u} \equiv [u_1, u_2, ..., u_N]$, $\underline{h} \equiv [h_1, h_2, ..., h_M]$ are the subsets of uknowns of the potential values at the nodes and of the interface location at the nodes along the interface, respectively; p is a relevant parameter. Here the parameter of importance is, of course, the strength of the applied magnetic field, H_0, or the applied magnetic induction $B_0 = \mu_0 H_0$.

At a given parameter value, $p = B_0$, the algebraic equation set is solved by Newton iteration:

$$\underline{\underline{J}}^{(k)} [\underline{y}^{(k+1)} - \underline{y}^{(k)}] = -\underline{R}^{(k)} \tag{11}$$

where k is the iteration counter, $\underline{y}^{(k)}$ is the approximation of the solution at the k-th iteration and $\underline{R}^{(k)}$ is the set of residuals calculated at $\underline{y} = \underline{y}^{(k)}$. Initial estimates, $\underline{y}^{(0)}$, of a solution at a given parameter value are provided by solutions already found at nearby parameter values, in the course of continuation in parameter space ([8]). $\underline{\underline{J}}^{(k)}$ is the Jacobian matrix,

$$J_{ij} = \partial R_i / \partial y_j \tag{12}$$

calculated at $\underline{y} = \underline{y}^{(k)}$.

$\underline{\underline{J}}$ is a sparse matrix, due to the limited overlap of the finite element basis functions over the domain. In block-notation $\underline{\underline{J}}$ is:

$$\underline{\underline{J}} = \begin{vmatrix} \dfrac{\partial \underline{R}_p}{\partial \underline{u}} & \dfrac{\partial \underline{R}_p}{\partial \underline{h}} & \underline{0} \\ \dfrac{\partial \underline{R}_{YL}}{\partial \underline{u}} & \dfrac{\partial \underline{R}_{YL}}{\partial \underline{h}} & \dfrac{\partial \underline{R}_{YL}}{\partial K} \\ 0 & \dfrac{\partial R_{VC}}{\partial \underline{h}} & 0 \end{vmatrix} \tag{13}$$

The off-diagonal blocks $[\dfrac{\partial \underline{R}_p}{\partial \underline{h}}]$, of size (N x M), and $[\dfrac{\partial \underline{R}_{YL}}{\partial \underline{u}}]$, of size (M x N), are not identical: in the former, Laplace's equation residuals depend on the interface location unknowns through the element boundaries that follow the interface shape; in the latter, the Young-Laplace equation residuals depend only on the potential unknowns at the nodes that belong to elements adjacent to the interface (since in Eqn. (4) the gradient of the potential is evaluated at z=h(r)). *Therefore* $\underline{\underline{J}}$ *is a non-symmetric matrix.*

At each iteration, the linearized equation set (11) is solved by a frontal solver ([9]), an implementation of Gauss elimination suitable for the direct solution of large and sparse equation systems. At a given value of the parameter p, the nonlinear equation set (10) can have a unique solution, or multiple solutions (when p is a bifurcation point), or even no solution (when p is a turning point on a solution branch). Solution multiplicity is monitored and entire solution branches are traced by parameter continuation.

Stability is governed by the minimization of the energy functional $\wp$ in Eqn. (8). Replacement of u and h in Eqn. (8) by their approximations from Eqns. (9) yields an expression $\wp = \wp(\underline{y}; p) = \wp(\underline{u}, \underline{h}, K; p)$ for the energy functional. The necessary condition for the minimization of $\wp$ is:

$$\frac{\partial \wp}{\partial \underline{y}} = \underline{0} \tag{14}$$

The solutions of Eqns. (14) are solutions of the magnetohysdrostatic equilibria of the ferrofluid interface and they should coincide with those of Eqns. (10), as expected by the equivalence of force and energy formulations.

Any admissible disturbance from an equilibrium solution is expressed in terms of the same finite element basis functions used for the approximation of the equilibrium solution (cf. Eqns. (9)). Thus the stability is governed by a generalized eigenproblem ([10])

$$\underline{\underline{H}} \underline{x}_i = \lambda_i \underline{\underline{M}} \underline{x}_i \tag{15}$$

where $\underline{\underline{H}}$ is the so-called Hessian, or stability matrix, of the energy formulation, $H_{ij} = \partial^2 \wp / \partial y_i \partial y_j$, and $\underline{\underline{M}}$ is the overlap or 'mass' matrix of the finite element basis functions, i.e. the inner products of basis functions. the Hessian and mass matrix in (15) are evaluated at equilibrium solutions. In block-notation $\underline{\underline{H}}$ is:

$$\underline{\underline{H}} = \begin{vmatrix} \dfrac{\partial^2 \wp}{\partial \underline{u} \partial \underline{u}} & \dfrac{\partial^2 \wp}{\partial \underline{u} \partial \underline{h}} & \underline{0} \\ \dfrac{\partial^2 \wp}{\partial \underline{h} \partial \underline{u}} & \dfrac{\partial^2 \wp}{\partial \underline{h} \partial \underline{h}} & \dfrac{\partial^2 \wp}{\partial \underline{h} \partial K} \\ 0 & \dfrac{\partial^2 \wp}{\partial K \partial \underline{h}} & 0 \end{vmatrix} \tag{16}$$

Eqn. (16) makes clear that $\underline{\underline{H}}$ *is a symmetric matrix.*

All the eigenvalues of the symmetric eigenproblem (15) are necessarily real; if any of the eigenvalues is negative, the equilibrium state is unstable to the corresponding eigenvector $\underline{x}_i$, that is to the disturbance 'carried' by the eigenvector. Therefore, among the eigenvalues those that change sign ('cross' zero) along a solution branch signal change of solution stability. Thus the eigenvalues to be monitored along an equilibrium solution branch (in the course of

parameter continuation) are those of the smallest magnitude. Because the eigenvalues of the standard eigenproblem

$$\underline{\underline{H}}\underline{x} = \lambda \underline{x} \tag{17}$$

and those of the generalized eigenproblem (15) cross zero simultaneously, it suffices to monitor the eigenvalues of smallest magnitude of (17). The equivalence of force and energy formulations in the continuum suggests that the eigenvalues of smallest magnitude of the standard eigenproblem

$$\underline{\underline{J}}\underline{x} = \lambda \underline{x} \tag{18}$$

be also monitored.

4 The Arnoldi and Lanczos Eigensolvers

When $\underline{\underline{A}}$ is a n x n non-symmetric matrix, as in the case $\underline{\underline{A}} = \underline{\underline{J}}$, the eigenproblem

$$\underline{\underline{A}}\underline{x} = \lambda \underline{x} \tag{19}$$

is solved here by Arnoldi's algorithm ([1], [11], [12]):

Choose $\underline{q}_1$ with $\|\underline{q}_1\| = 1$
For j = 1 **until** Convergence **Do**
1. Compute and store $\underline{\underline{A}}\underline{q}_j$
2. Compute $h_{t,j} = (\underline{\underline{A}}\underline{q}_j, \underline{q}_t)$ $t = 1, \ldots, j$
3. $\underline{r}_j = \underline{\underline{A}}\underline{q}_j - \sum_{t=1}^{j} h_{t,j}\underline{q}_t$
4. $h_{j+1,j} = (\underline{r}_j, \underline{r}_j)^{1/2}$
5. $\underline{q}_{j+1} = \underline{r}_j / h_{j+1,j}$

End For

At step j, the algorithm produces an orthonormal basis $\{\underline{q}_1, \underline{q}_2, \ldots, \underline{q}_m\}$ of the Krylov subspace $\mathbf{K}_j$ spanned by $\underline{q}_1, \underline{\underline{A}}\underline{q}_1, \ldots, \underline{\underline{A}}^{j-1}\underline{q}_1$. The projection of $\underline{\underline{A}}$ on $\mathbf{K}_j$ is represented in the basis $\{\underline{q}_i\}$ by the upper Hessenberg matrix $\underline{\underline{H}}_j = \underline{\underline{Q}}_j^T \underline{\underline{A}} \underline{\underline{Q}}_j$, whose elements are the coefficients h_{ij}. The eigenvalues of $\underline{\underline{H}}_j$ provide approximations of the eigenvalues of $\underline{\underline{A}}$ only for the outermost part of the spectrum of $\underline{\underline{A}}$, whereas the inner eigenpairs are poorly represented. The eigenproblem for $\underline{\underline{H}}_j$ is small and it is solved routinely by EISPACK.

When $\underline{\underline{A}}$ is a n x n symmetric matrix, as in the case $\underline{\underline{A}} = \underline{\underline{H}}$, Lanczos' algorithm ([13], [14]) is preferred for the solution of (19):

$\underline{v}_i := 0$ $i = 1, 2, \ldots, n$
$\beta_0 := 1$
$j := 0$
Do While $(\beta_j \neq 0)$
  If $(j \neq 0)$ then
    For $i = 1, \ldots, n$
      $t := \underline{w}_i$, $\underline{w}_i := \underline{v}_i / \beta_j$, $\underline{v}_i := -\beta_j \underline{t}$
  $\underline{v} := \underline{\underline{A}}\underline{w} + \underline{v}$
  $j := j + 1$
  $a_j := (\underline{w}, \underline{v})$
  $\underline{v} := \underline{v} - a_j \underline{w}$
  $\beta_j := \|\underline{v}\|$

The extreme eigenvalues and the corresponding eigenvectors of $\underline{\underline{A}}$ are approximated by the eigenvalues of the symmetric tridiagonal matrix $\underline{\underline{T}}_j$ whose diagonal and subdiagonal elements are $a_1, \ldots, a_j$ and $\beta_1, \ldots, \beta_{j-1}$, respectively. The eigenproblem for $\underline{\underline{T}}_j$ is solved with EISPACK, as before.

5 Stability analysis: results and discussion

Theoretical predictions were computed at the following parameter values: $\chi \equiv (\mu/\mu_0)-1 = 1$, $\Delta\rho = 792$ kg/m^3 and $\sigma = 0.029$ N/m. The computational domain was half of that shown in Figure 1, the one to the right of the symmetry axis at r=0, due to the axial symmetry of the solutions sought; it was tessellated finely enough that the solutions of the discretized governing equations are reliable, i.e. robust against further discretization refinement. 20 elements were placed in the vertical direction and 10 in the radial -- a total of 200 elements. The total number of unknowns (and thus of equations) was 883. The discretization used was judged appropriate to guarantee reliability of solutions: doubling the number of elements led to solutions that were close to within 1.5% to the ones already obtained. The governing equations as well as the corresponding residual equations admit a flat solution at *all* values of applied field strength:

flat interface: $h = 0$,
linear magnetostatic potential:
$u_a = (B_0/\mu_0)(z + D_2/(\chi+1))$, $u_b = (B_0/\mu)(z + D_2)$,
reference pressure $K = \frac{1}{2} B_{0}^2 \chi/\mu$

The eigenvalues of smallest magnitude (usually 5 to 10 in number) of $\underline{\underline{J}}$ and $\underline{\underline{H}}$ are monitored along the flat solution branch by continuation in the value of B_0. Arnoldi's eigensolver is used for $\underline{\underline{J}}$ and Lanczos' for $\underline{\underline{H}}$. The determinant of $\underline{\underline{J}}$ and $\underline{\underline{H}}$ is also monitored. The eigenvalues of smallest magnitude are computed most conveniently by incorporating the inverse power method in the eigensolvers ([1], [13]). This requires inversion of $\underline{\underline{J}}$ and $\underline{\underline{H}}$ (instead of a matrix-vector multiplication -- the case when the eigenvalues of

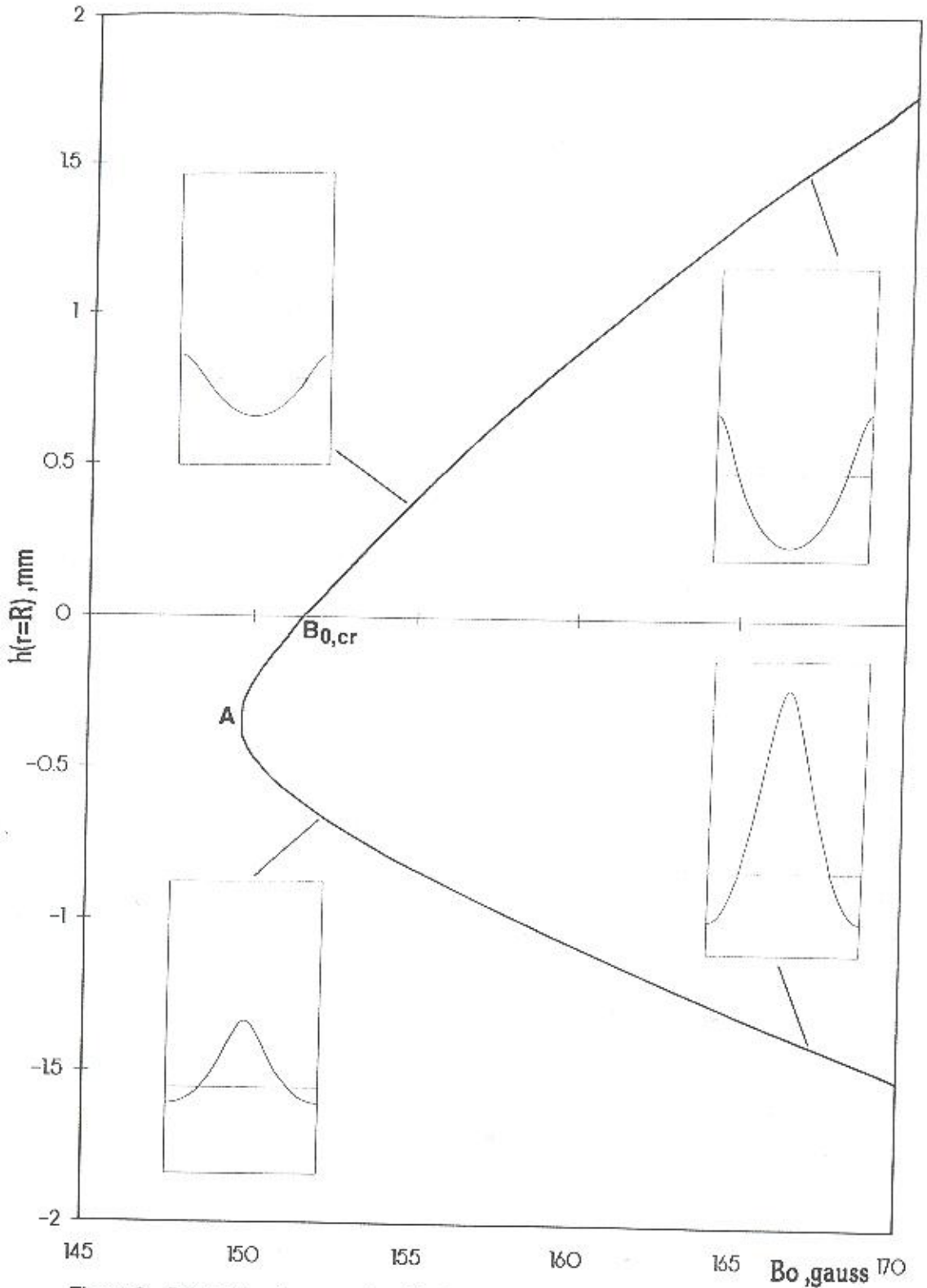

Figure 2: Bifurcation diagram of equilbrium axisymmetric shapes of ferrofluid interface in magnetic field ($B_0=\mu_0 H_0$)

largest magnitute are wanted; cf. Section 4). Inversion, however, is not actually needed because it is already done by frontal solver for solving the linearized set of governing equations during Newton iteration (Eqn. (11)); what needed to be done was simply the implementation of a 'communication interface' between Arnoldi's and Lanczos' solvers and the re-solution part of the frontal solver (the subroutine that re-solves $\underline{\underline{J}}\underline{x} = \underline{b}$, or $\underline{\underline{H}}\underline{x} = \underline{b}$, when $\underline{\underline{J}}$ or $\underline{\underline{H}}$ are already inverted and $\underline{b}$ changes).

The flat solution becomes unstable to axisymmetric disturbances of the interface shape beyond a critical magnetic induction strength, $B_{0,cr}$ ($H_{0,cr}=B_{0,cr}/\mu_0$). The predicted critical value of B_0 at the onset of the instability was $B_{0,cr}=150.842$ gauss and agrees, within 0.2%, with predictions of linearized theory ([4]). At the parameter value $B_0=B_{0,cr}$ a bifurcation point appears on the branch representing the flat solution. Across the bifurcation point on the flat solution the determinant of $\underline{\underline{J}}$ and of $\underline{\underline{H}}$ change sign indicating that an odd number of eigenvalues of $\underline{\underline{J}}$ and $\underline{\underline{H}}$ change sign. Arnoldi's and Lanczos' eigensolvers find sign change of one eigenvalue.

The bifurcation of equilibrium solutions with distorted interface shape from the flat solution branch is shown in Figure 2; their branch is hereafter called distorted solution branch. The bifurcation is two-sided (or trans-critical), that is distorted solutions exist near criticallity at parameter values higher and lower than $B_0=B_{0,cr}$. The eigenvector $\underline{x}$ corresponding to the eigenvalue that crosses zero is an axisymmetric disturbance that gives way to axisymmetric equilibrium solutions with distorted interface shape emanating from the flat solution branch. The interface shape in the eigenvector is shown in Figure 3a. Initial estimates, $\underline{y}_d^{(0)}$, of solutions on the distorted solution branch are provided by $\underline{x}$:

$$\underline{y}_d^{(0)} = \underline{y}_f + \varepsilon \underline{x} \qquad (20)$$

where $\underline{y}_f$ is a solution on the flat solution branch at $B_0=B_{0,cr}$ and ε is a small amplitude parameter.

Sample interface shapes on the distorted solution branch are shown in Figure 2. On the supercritical part of the branch ($B_0>B_{0,cr}$) the deflection of the interface is negative at the axis of symmetry (r=0). On the subcritical part a spike develops at the axis of symmetry. The subcritical part of the distorted solution branch 'turns back' towards values of B_0 higher than the critical at a turning point A, where $B_0=B_{0,A}=148.2$ gauss (see Figure 2); that is, distorted interface shapes with a spike at r=0 fail to exist at $B_0<B_{0,A}$. The turning point is cirmumvented during parameter continuation by employing arc-length-type continuation methods ([8]).

The stability of solutions along the flat and the distorted solution branches is determined by the sign

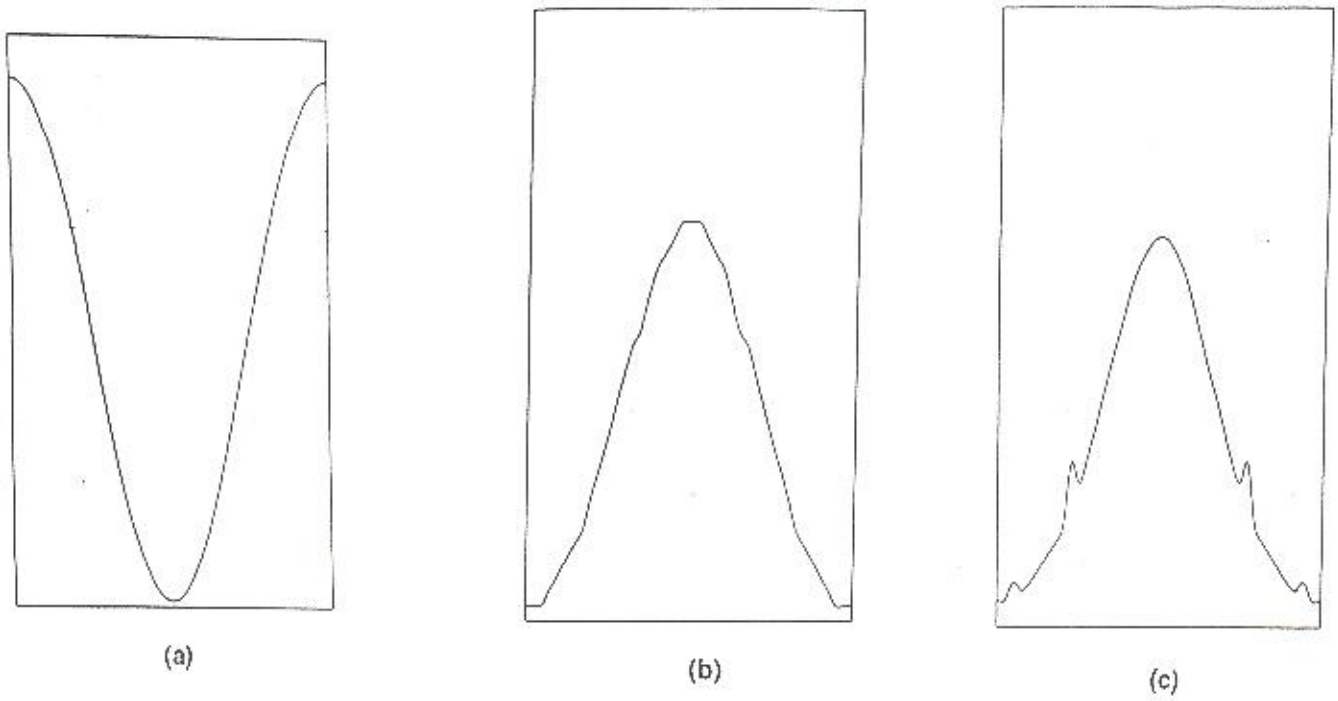

Figure 3: Interface shape in the eigenvectors: (a) on the flat branch at $B_0=B_{0,cr}$; (b) on the bifurcating branch of distorted interface shapes at $B_0=B_{0,cr}$; (c) close to the turning point A

of the eigenvalues of the eigenproblem (15). Stability of solutions changes when a positive eigenvalue turns negative. This happens along the flat solution branch across $B_0=B_{0,cr}$ and along the distorted solution branch across $B_0=B_{0,cr}$ and $B_0=B_{0,A}$. Equilibrium solutions on the flat solution branch are stable at $0<B_0<B_{0,cr}$ and unstable at $B_0>B_{0,cr}$. Solutions on the supercritical part of the distorted solution branch are stable; on the subcritical part solutions are unstable at $B_{0,A}<B_0<B_{0,cr}$ but they regain stability past the turning point (at $B_0>B_{0,A}$). The stability results predicted here agree with those dictated by elementary stability and bifurcation theory ([15]). The interface shape in the eigenvectors corresponding to the eigenvalues that change sign on the distorted solution branch across $B_0=B_{0,cr}$ and across $B_0>B_{0,A}$ are shown in Figures 3b and 3c, respectively.

Stability predictions of Arnoldi's and Lanczos' methods are practically identical. However Lanczos' method is superior to Arnoldi's in terms of computational cost: as shown in Figure 4a, for a reasonable size of the matrix ($\underline{J}$ and $\underline{\underline{H}}$), Arnoldi's eigensolver is about three times more expensive than Lanczos'. Performance diagrams of Arnoldi's and Lanczos' eigensolvers are shown in Figures 4b, 4c and 4d. At fixed number of Arnoldi steps, the computational cost grows sharply, although linearly, with the number of wanted eigenvalues (Figure 4b). Cost drops linearly with the number of Arnoldi steps, at fixed number of wanted eigenvalues, up to about 15 steps (Figure 4c). Figure 4d shows that the cost of Lanczos' eigensolver grows almost linearly with the number of wanted eigenvalues.

References

1. Christodoulou, K. N. and Scriven, L. E. (1988) Finding Leading Modes of a Viscous Free Surface Flow: An Asymmetric Generalized Eigenproblem. *J. Sci. Comp.*, Vol. 3, 355-406.

2. Cowley, M. D. and Rosensweig, R. E. (1967) The Interfacial Stability of a Ferromagnetic Fluid. *J. Fluid Mech.*, Vol. 30, 671-688.

3. Rosensweig, R. E., Ferrohydrodynamics. Cambridge University Press, Cambridge, 1985.

4. Boudouvis, A. G. (1987) Mechanisms of Surface Instabilities and Pattern Formation in Ferromagnetic Liquids. Ph.D. Thesis, University of Minnesota, Minneapolis, USA.

5. Strang, G. and Fix, G. J., An Analysis of the Finite Element Method. Prentice-Hall, Englewood Cliffs, New Jersey, 1973.

6. Boudouvis, A. G., Puchalla, J. L. and Scriven, L. E. (1988) Interaction of Capillary Wetting and Fringing Magnetic Field in Ferrofluid Systems. *J. Colloid Interface Sci.*, Vol. 124, 677-687.

7. Boudouvis, A. G., Puchalla, J. L. and Scriven, L. E. (1988) Magnetohydrostatic Equilibria of

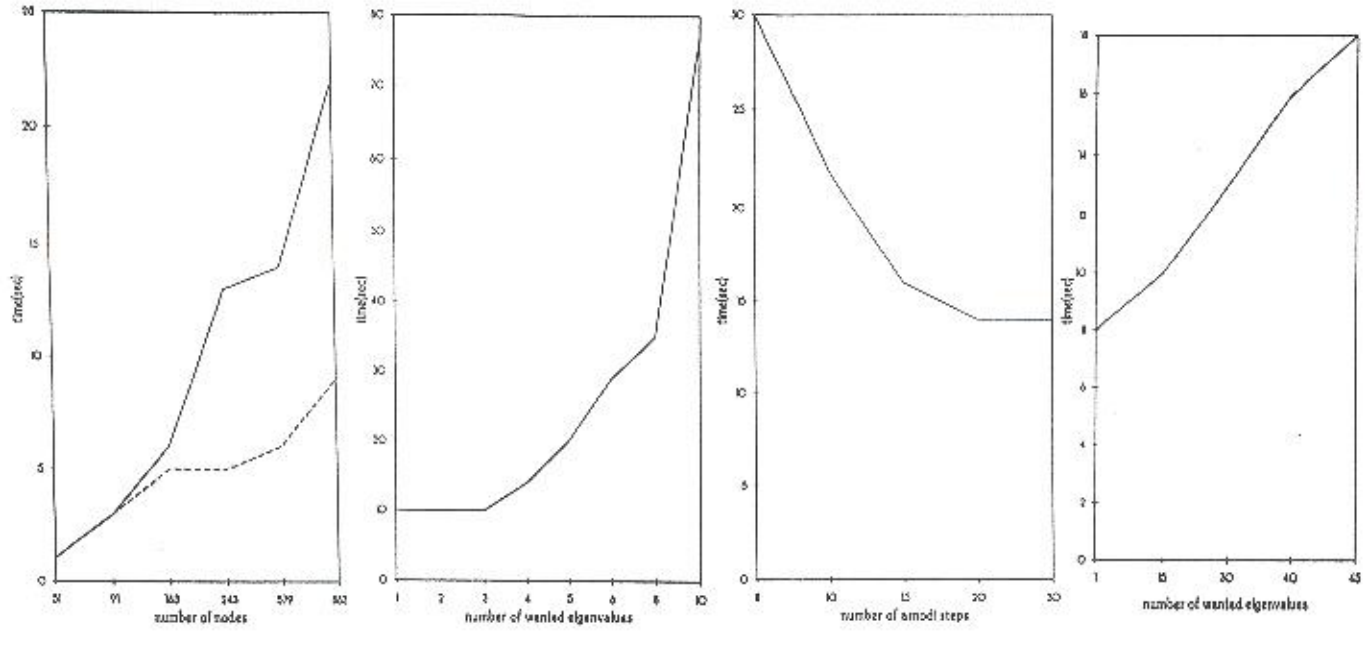

Figure 4: Performance diagrams of Lanczos' and Arnoldi's eigensolvers. (a) 4 wanted eigenvalues; — Arnoldi with 10 steps --- Lanczos. (b) Arnoldi with 20 steps; matrix size 883 x 883. (c) Arnoldi with 4 wanted eigenvalues; matrix size 883 x 883. (d) Lanczos; matrix size 883 x 883

Ferrofluid Drops in External Magnetic Fields. *Chem. Eng. Comm.*, Vol. 67, 129-144.

8. Keller, H. B., Numerical Solution of Bifurcation and Nonlinear Eigenvalue Problems. In *Applications of Bifurcation Theory* (P. H. Rabinowitz, ed.), pp. 359-384, Academic Press, New York, 1977.

9. Hood, P. (1976) Frontal Solution Program for Unsymmetric Matrices. *Int. J. Num. Meth. Engng.*, Vol. 10, 379-399.

10. Brown, R. A. and Scriven, L. E. (1980) The Shapes and Stability of Captive Rotating Drops. *Phil. Trans. R. Soc. Lond.*, Vol. 297, 51-79.

11. Saad, Y. (1980) Variations of Arnoldi's Method for Computing Eigenelements of Large Unsymmetric Matrices. *Lin. Alg. Appl.*, Vol. 34, 269-295.

12. Kim, S. K. and Chronopoulos, A. T. (1992) An Efficient Parallel Algorithm for Extreme Eigenvalues of Sparse Nonsymmetric Matrices. *Int. J. Supercomp. Appl.*, Vol. 6, 98-111.

13. Parlett, B. N., The Symmetric Eigenvalue Problem. Prentice-Hall, Englewood Cliffs, New Jersey, 1980.

14. Scott, D. S., Block Lanczos Software for Symmetric Eigenvalue Problems. Report CSD-48, Oak Ridge National Laboratory, 1979.

15. Iooss, G. and Joseph, D. D., Elementary Stability and Bifurcation Theory. Springer-Verlag, New York,1980.